## **Supplementary Information for**

# Interannual fires as a source for subarctic summer decadal climate variability mediated by permafrost thawing

#### **Authors**

Ji-Eun Kim\*a,b, Ryohei Yamaguchi<sup>c</sup>, Keith B. Rodgersa,b, Axel Timmermanna,b, Sun-Seon Leea,b, Karl Steina,b, Gokhan Danabasoglud, Jean-Francois Lamarqued, John T. Fasullod, Clara Deserd, Nan Rosenbloomd, Jim Edwardsd, Malte F. Stueckere

#### **Affiliations**

<sup>a</sup>Center for Climate Physics, Institute for Basic Science, Busan, South Korea.

<sup>b</sup>Pusan National University, Busan, South Korea.

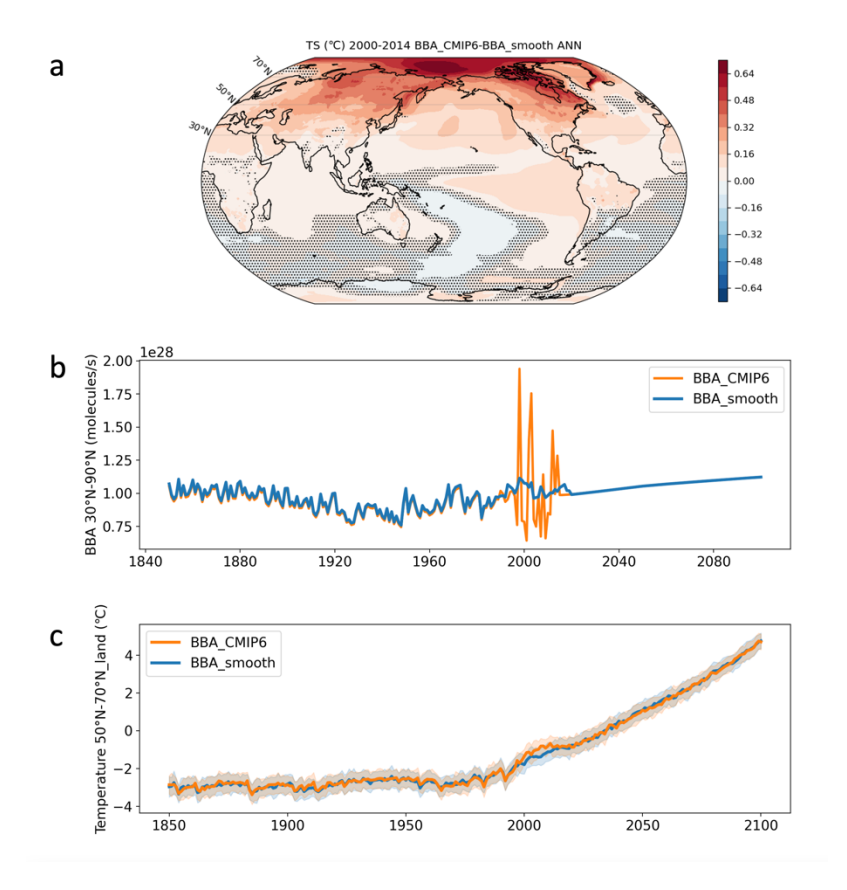
<sup>c</sup>Research Institute for Global Change, Japan Agency for Marine-Earth Science and Technology, Yokosuka, Japan.

<sup>d</sup>National Center for Atmospheric Research, Boulder, CO, USA.

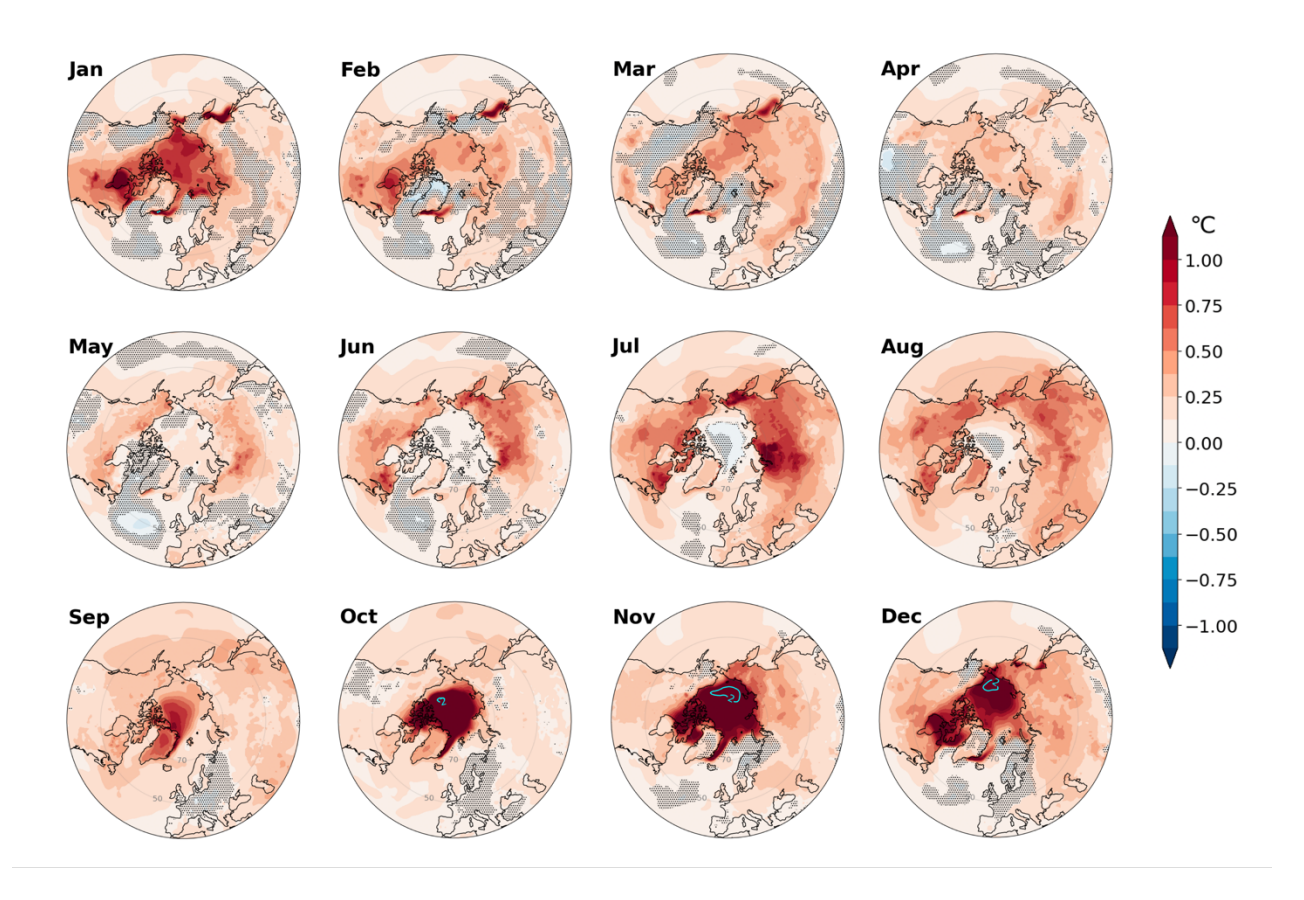
<sup>e</sup>Department of Oceanography and International Pacific Research Center, School of Ocean and Earth Science and Technology, University of Hawai'i at Mānoa, Honolulu, HI, USA.

\*Correspondence to: jieunkim@pusan.ac.kr

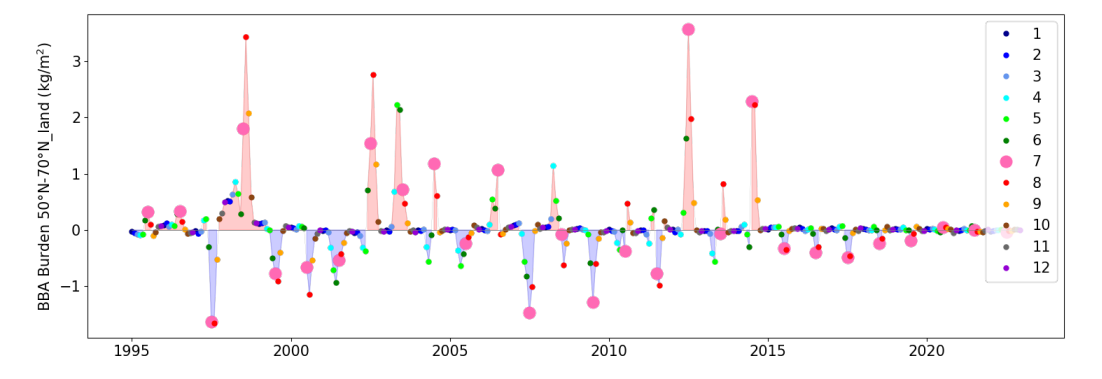
npj Climate and Atmospheric Science



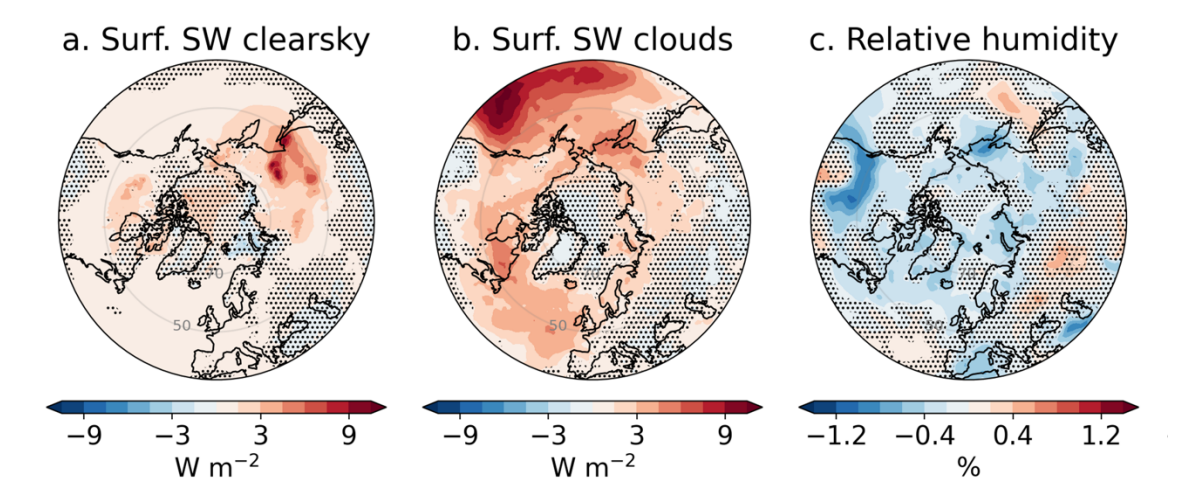
Supplementary Figure 1. Decadal mean surface temperature response to interannually varying BBA emissions. (a) Mean annual surface temperature difference (BBA\_CMIP6 – BBA\_smooth) for 2000-2014. Stippling denotes non-significant areas whose values are within one standard deviation of the internal variability range (see Methods). (b) Time series of 30°N-90°N annual BBAs prescribed in BBA\_CMIP6 (orange) and BBA\_smooth (blue) simulations. (c) Time series of annual temperature over the land domain between 50°N-70°N for the two ensemble groups. Shading represents one standard deviation from 50 ensemble members for each group.



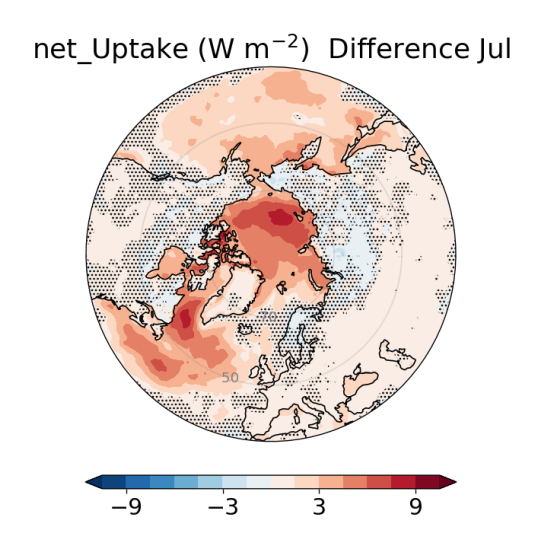
**Supplementary Figure 2. Regionally and seasonally distinct decadal temperature responses.** Surface temperature differences between the two ensemble groups (BBA\_CMIP6 – BBA\_smooth) over 2000-2014 for each month. The cyan contour corresponds to 2°C. Stippling denotes non-significant areas (see Methods).



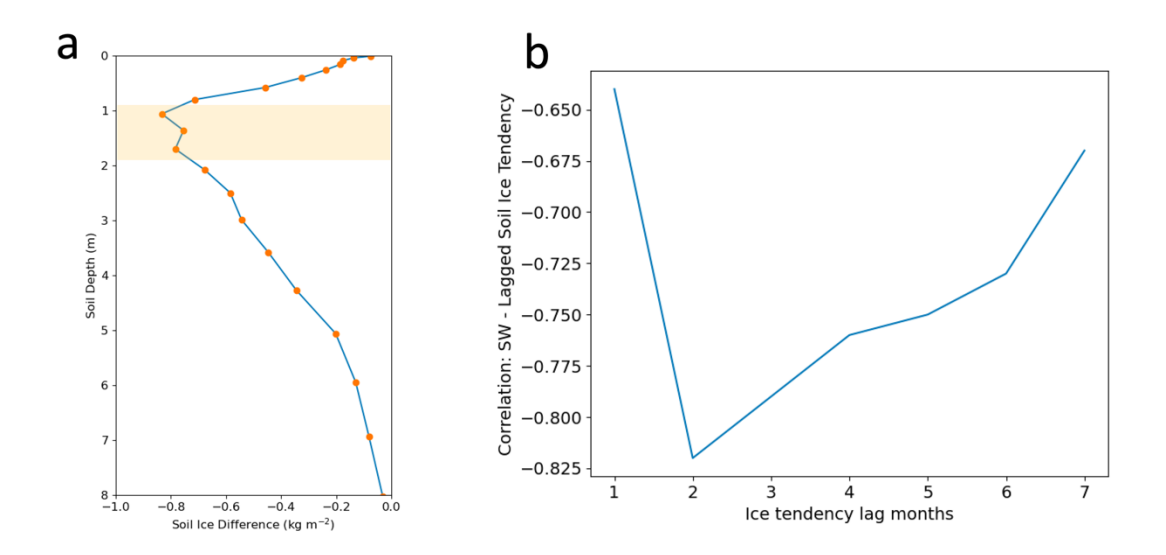
**Supplementary Figure 3. Monthly evolution of differences (BBA\_CMIP6 – BBA\_smooth) in atmospheric BBA burden.** Monthly time series of BBA column burden differences over the land domain between 50°N-70°N. Dot colors denote months as in Fig. 1a.



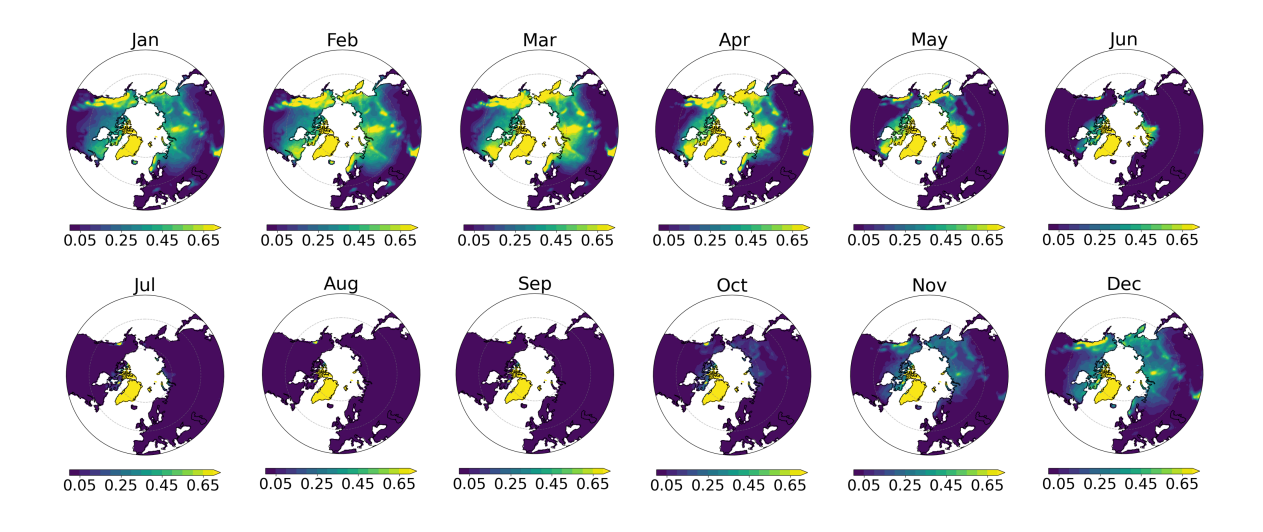
**Supplementary Figure 4. Aerosol direct and indirect effects.** Composites of 8 low BBA emission years (1997, 1999, 2000, 2001, 2005, 2007, 2009, 2011) minus composites of 4 high emission years (1998, 2002, 2003, 2012) in BBA\_CMIP6 for (a) clear-sky shortwave flux at the surface, (b) changes in surface shortwave flux by clouds, and (c) low-level (> 700 hPa) relative humidity. The downward direction is positive for (a) and (b). The selected composite years are the same as in Fig. 1c-f, and all values are for MJJAS. Stippling denotes non-significant areas (see Methods).



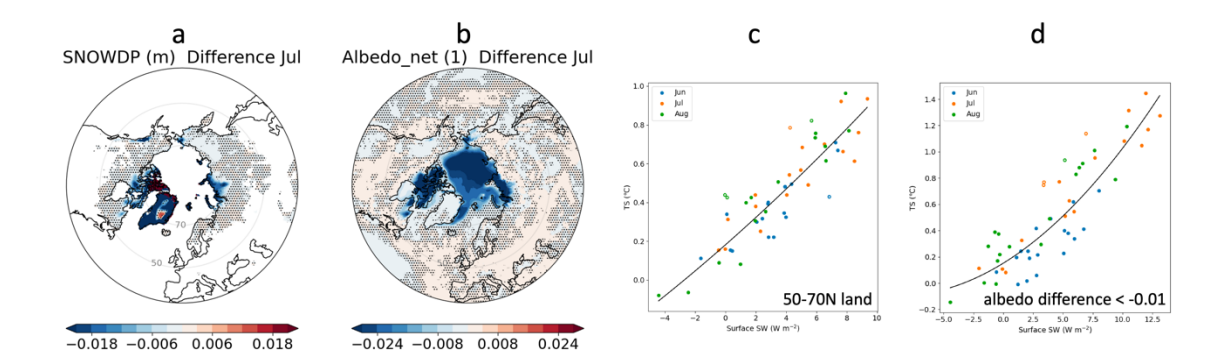
Supplementary Figure 5. July difference (BBA\_CMIP6 – BBA\_smooth) map of net heat uptake at the surface averaged over 2000-2014. The net heat uptake is estimated as residuals of net surface shortwave, longwave, sensible heat, and latent heat fluxes. Positive values represent anomalous heat entering (downward) the surface, and stippling denotes non-significant areas (see Methods).



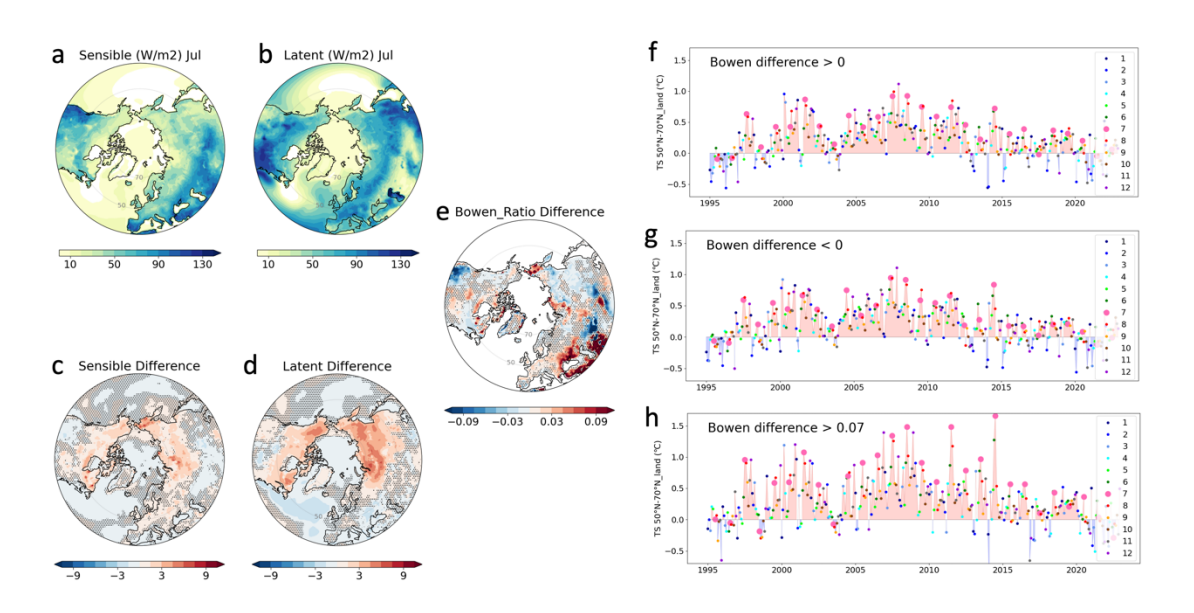
**Supplementary Figure 6. Soil ice melting in response to increases in surface shortwave flux.** (a) Anomalous soil ice in BBA\_CMIP6 relative to BBA\_smooth as a function of depth. The orange dots correspond to soil model layers in CLM5<sup>1</sup>. The largest ice melting occurs at depth between 0.9-1.9 m (shading). (b) Correlation coefficients between net surface shortwave flux and soil ice tendency at soil layers of 0.9-1.9 m as a function of lag month.



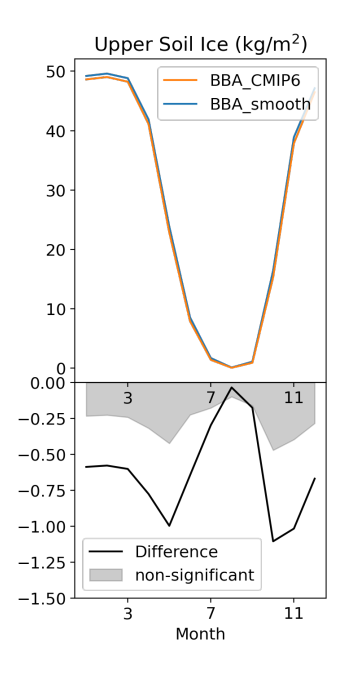
Supplementary Figure 7. Monthly mean snow cover for 2000-2014 in BBA smooth.



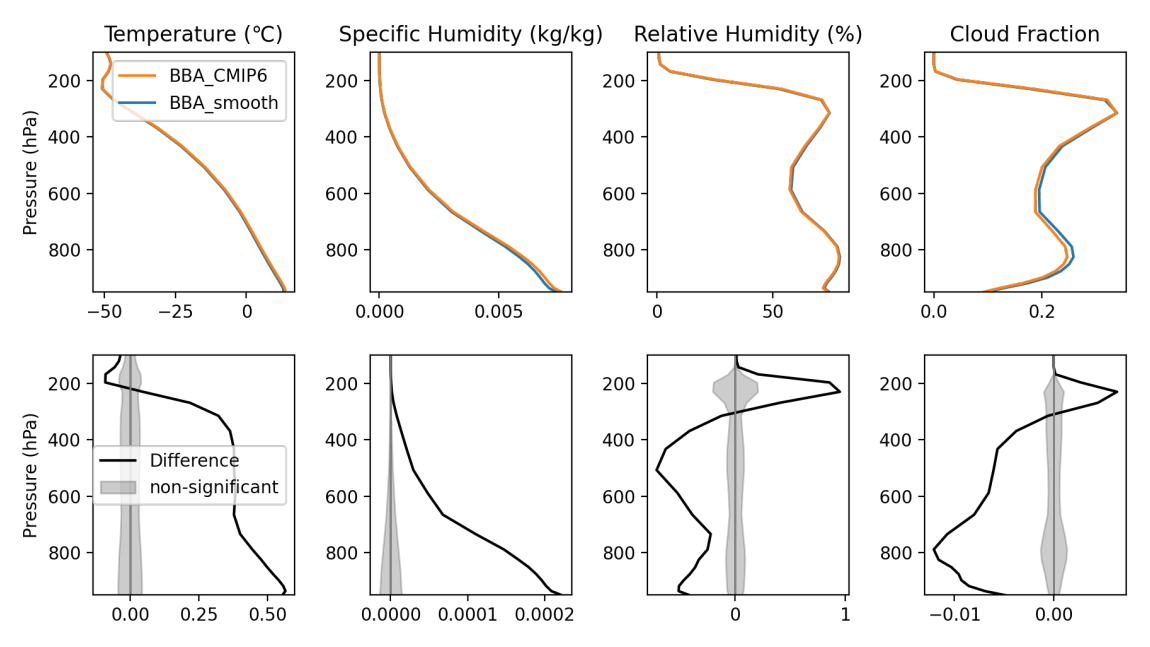
**Supplementary Figure 8. Snow cover and albedo feedback.** July difference (BBA\_CMIP6 – BBA\_smooth) maps of (a) snow depth and (b) albedo. Stippling denotes non-significant areas (see Methods). Relationship between net surface shortwave flux and surface temperature averaged over (c) 50°N-70°N land and (d) areas where albedo difference < -0.01. For scatters and the polynomial fit in (c-d), the same methods are used as for Fig. 3a-d.



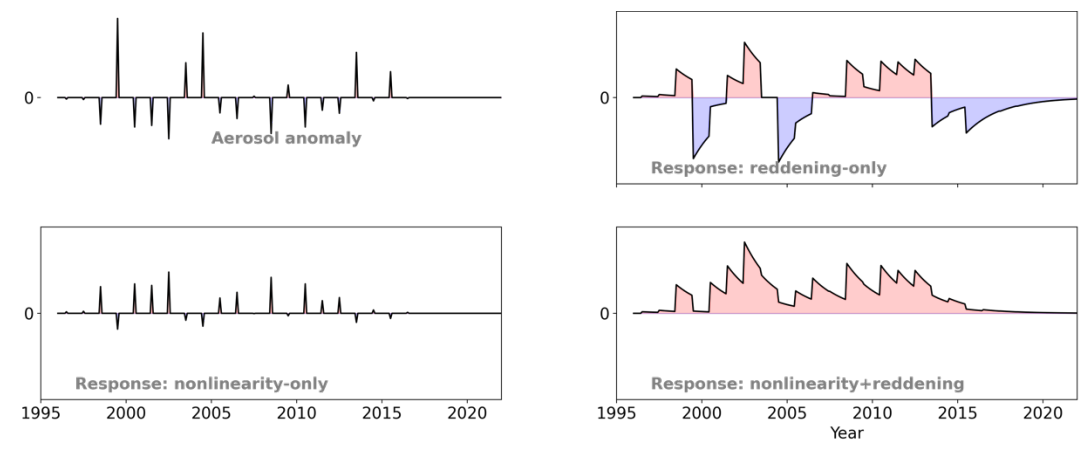
**Supplementary Figure 9. Sensible and latent heat fluxes, and their impact on surface temperature.** The mean (a) sensible and (b) latent heat flux in BBA\_smooth, and differences (BBA\_CMIP6 – BBA\_smooth) of (c) sensible and (d) latent heat flux, and (e) Bowen ratio (sensible to latent heating). Monthly time series of surface temperature over areas where (f) Bowen ratio > 0, and (g) Bowen < 0, and (h) Bowen ratio > 0.07 over 50°N-70°N land. Dot colors denote months.



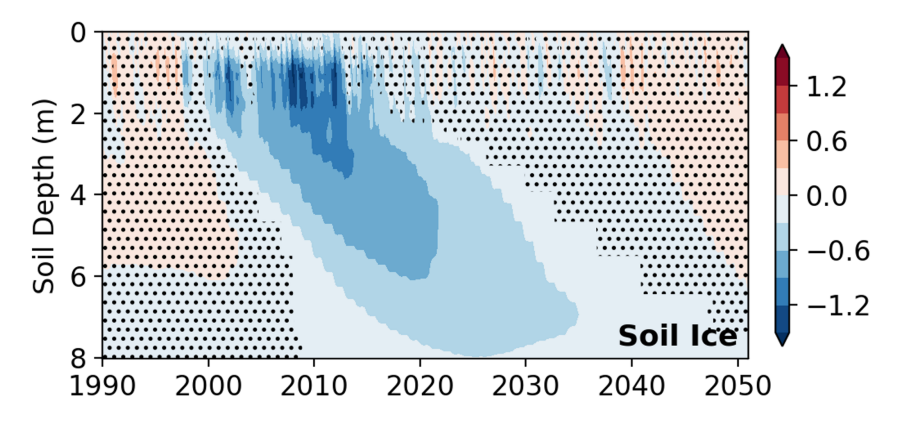
Supplementary Figure 10. Annual cycle of upper 12 cm soil ice in BBA\_CMIP6 (orange) and BBA\_smooth (blue), and their difference (black) over 50°N-70°N for 2000-2014. The grey shading represents ranges of non-significant values (see Methods).



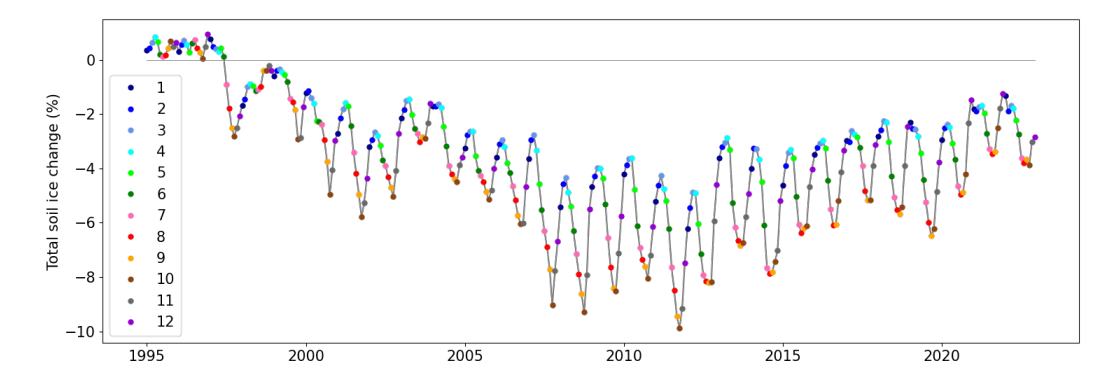
Supplementary Figure 11. Atmospheric responses in July over the land domain between 50°N-70°N for 2000-2014. Vertical profiles (left to right) of temperature, specific humidity, relative humidity, and cloud fraction for BBA\_CMIP6 (orange) and BBA\_smooth (blue), and their differences (black). The grey shading represents ranges of non-significant values (see Methods).



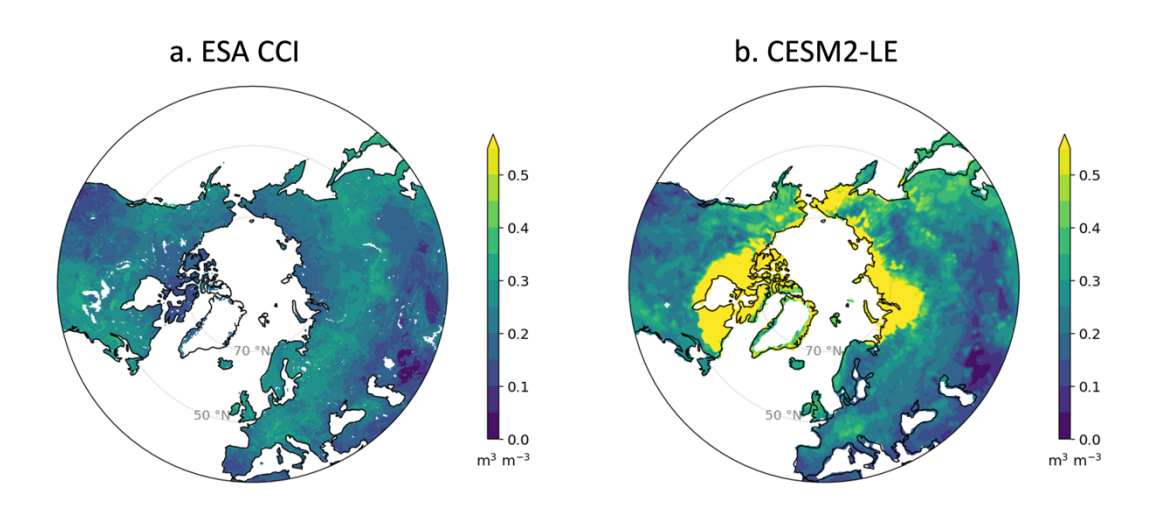
Supplementary Figure 12. Three conceptual model responses to (upper left) aerosol fluctuations in BBA\_CMIP6 – BBA\_smooth. (lower left) A response varies at the same interannual timescale as the emission timescale when there is only nonlinearity in atmospheric processes. (upper right) A response fluctuates interannually with a gradual decay of a signal (reddening) after a symmetric linear response to an aerosol pulse when a climate system has a memory effect. The decay timescale of 2 years is used in this example. (lower right) When both nonlinearity and reddening are present, a response is similar to the temperature response shown Fig. 2e. The upper left aerosol anomalies are estimated from annual mean BBA differences between BBA\_CMIP6 and BBA\_smooth, and the time-integrated value is set to zero. Units are arbitrary.



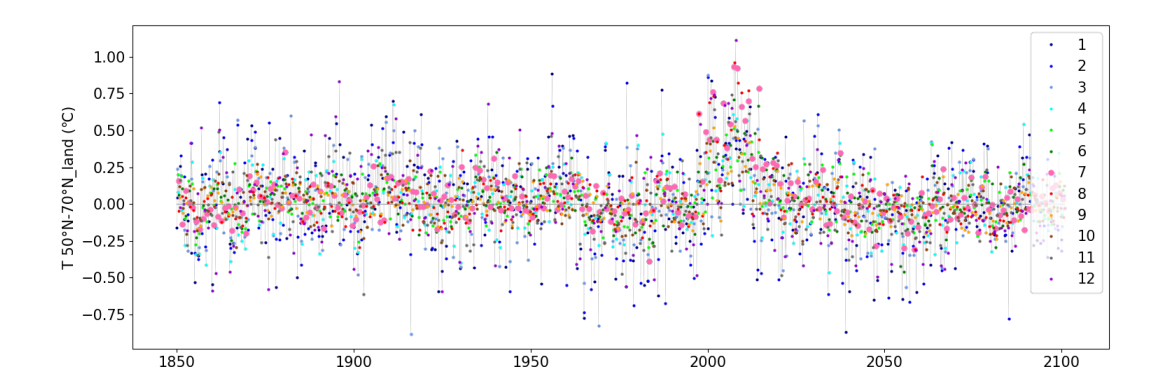
Supplementary Figure 13. Same as Fig. 2b, but for an extended period. Unit is kg m<sup>-2</sup>.



**Supplementary Figure 14. Loss of soil ice.** Percentage change of vertically-integrated soil ice over the entire model layer (up to 8.6 m depth <sup>1</sup>) in BBA\_CMIP6 relative to BBA\_smooth over 50°N-70°N, with colors distinguishing months.



**Supplementary Figure 15. Surface soil moisture.** Mean July volumetric surface soil moisture (m³ m⁻³) in (a) the observation-based ESA CCI data product and (b) CESM2-LE averaged over 1997-2014. The ESA CCI data product is representative of the first few centimeters of soil (surface to ~5 cm) and CESM2-LE values are calculated for the first two CLM5 model soil layers (surface to ~6 cm).



Supplementary Figure 16. Monthly time series of surface temperature difference (BBA\_CMIP6 – BBA\_smooth) over the land domain between 50°N-70°N for the period of 1850-2100. Surface temperature differences between the two 50-member ensemble groups nevertheless exhibit residuals even before 1990 due to non-zero cancellation of internal variability. Colors denote different months.

### **Supplementary Reference**

Lawrence, D. M. *et al.* The Community Land Model Version 5: Description of New Features, Benchmarking, and Impact of Forcing Uncertainty. *J. Adv. Model. Earth Syst.* **11**, 4245-4287 (2019).